Journal of Applied Physics

Core/shell/shell-structured nickel/carbon/polyaniline nanocapsules with large absorbing bandwidth and absorber thickness range

Cite as: J. Appl. Phys. **115**, 17A507 (2014); https://doi.org/10.1063/1.4861581
Submitted: 21 September 2013 . Accepted: 16 October 2013 . Published Online: 22 January 2014

Xianguo Liu, Siu Wing Or, Chung Ming Leung, and S. L. Ho

Core/shell/shell-structured nickel/carbon/polyaniline nanocapsules with large absorbing bandwidth and absorber thickness range

Xianguo Liu, Siu Wing Or,[a] Chung Ming Leung, and S. L. Ho
Department of Electrical Engineering, The Hong Kong Polytechnic University, Hung Hom, Kowloon, Hong Kong

(Presented 6 November 2013; received 21 September 2013; accepted 16 October 2013; published online 22 January 2014)

Core/shell/shell-structured nickel/carbon/polyaniline nanocapsules are prepared by a modified arc-discharge method and a chemical polymerization method, and their microwave absorbing properties are evaluated in the 2–18 GHz range covering the full S–Ku bands of microwaves. The bandwidth-broadening effect in various core/shell/shell material phases of the nanocapsules leads to Debye-type multidielectric polarizations in complex permittivity, a broad magnetic natural resonance of 2–8 GHz in complex permeability as well as extended absorbing bandwidth and absorber thickness range. A 3 mm-thick paraffin-bonded nanocapsule absorber shows an optimal reflection loss (RL) of −9.3 dB at 6.2 GHz with an extremely broad −5 dB-bandwidth of 3.4–18 GHz in almost the whole S–Ku bands as well as a very large absorber thickness range of down to 1 mm without deteriorating RL by 10%. © *2014 AIP Publishing LLC*. [http://dx.doi.org/10.1063/1.4861581]

Core/shell-structured nanocapsules, composed of a magnetic nanoparticle core (Ni, FeNi, etc.) and a dielectric shell (C, ZnO, AlO, CuO, etc.) in the nanometer size range, have been a main research focus for microwave absorbers in recent years.[1–5] However, the reported nanocapsules (Ni/C, FeNi/C, Ni/ZnO, Ni/AlO, Ni/CuO, etc.) mainly exhibit strong absorptions in high-frequency bands of microwaves (10–18 GHz in the X and Ku bands) with narrow absorbing bandwidths (<8 GHz) and large variations in absorption with absorber thickness (>10% for a change in absorber thickness by 10%) due to the limited material-phase variety constrained by their single core/shell structure.[1–5] In this work, we demonstrate the use of "core/multishell" structure in nanocapsules to broaden the absorbing bandwidth and absorber thickness range by the bandwidth-broadening effect in various core/multishell material phases. Accordingly, core/shell/shell-structured nanocapsules having a nickel (Ni) magnetic nanoparticle core, a first carbon (C) dielectric shell, and a second polyaniline (PANI) conducting polymer shell are prepared and their microwave absorbing properties are investigated.

A modified arc-discharge method was used to synthesize Ni/C nanocapsules.[1,2] A Ni ingot of 99.9% purity was placed in a water-cooled C crucible as the anode, while a C needle was employed as the cathode. After the arc-discharge chamber was evacuated to 5 mPa, 40 ml of liquid ethanol was introduced into the chamber filled with pure argon and hydrogen at 16 and 4 kPa, respectively. An arc-discharge current of 100 A was applied to the chamber for 8 h to ensure a sufficient evaporation of the Ni ingot. The Ni/C product, after being passivated in pure argon for 24 h, was collected from depositions on top of the chamber.

A chemical polymerization method was adopted to coat the second PANI shell on the Ni/C nanocapsules.[6] The as-synthesized Ni/C product was dispersed in 0.1 mol/l of hydrochloric acid (HCl) aqueous solution under ultrasonic vibrations for 30 min to remove oxides if present. The surface-cleaned Ni/C product was modified by a chemical graft procedure before being dispersed in 0.1 mol/l of 4-aminobenzoic acid (ABA) alcohol solution under stirring at 50 °C for 1 h. The ABA-grafted Ni/C product was put in 0.50 mol/l of HCl aqueous solution of aniline (ANI) with a pH value of 2 under ultrasonic vibrations for 1 h. 1 mol/l of ammonium peroxodisulfate (APS) aqueous solution was added into the dispersoid under stirring at 0 °C for 2 h. After the mixture was further stirred for 4 h, a chemical oxidative polymerization of ANI was carried out to obtain HCl-protonated PANI in which a polymerization reaction of the grafted amine of ABA and ANI occurred. The resulting Ni/C/PANI product was filtered by a magnetic separation process and washed several times with deionized water before being dried at 60 °C for 24 h.

The morphology and microstructure of the Ni/C and Ni/C/PANI products were observed by a high-resolution transmission electron microscopy (HRTEM) technique on a transmission emission microscope (JEOL 2010) with an emission voltage of 200 kV. Paraffin-bonded Ni/C/PANI nanocapsule absorbers were fabricated using 40 wt. % Ni/C/PANI nanocapsules. The S-parameters of the Ni/C/PANI absorbers were measured at different thicknesses (d) by a transmission/reflection coaxial line method in the 2–18 GHz frequency (f) range covering the whole S–Ku bands of microwaves using an S-parameter vector network analyzer (Agilent 8722ES). The f dependence of complex relative permittivity ($\varepsilon_r = \varepsilon_r' - j\varepsilon_r''$) and complex relative permeability ($\mu_r = \mu_r' - j\mu_r''$) at various d were converted from the measured S-parameter responses using the Nicolson-Ross-Weir conversion method. The f dependence of reflection loss (RL) at various d were deduced from the measured ε_r and μ_r spectra using[1–5]

[a]Author to whom correspondence should be addressed. Electronic mail: eeswor@polyu.edu.hk.

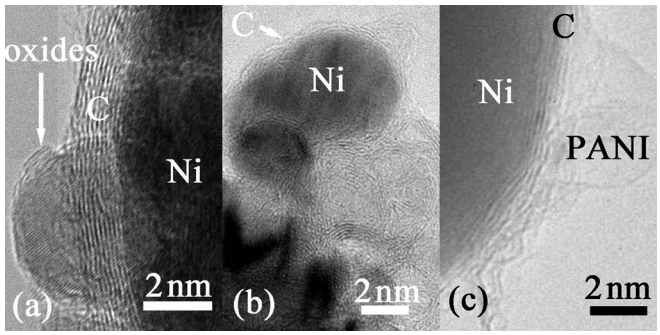

FIG. 1. HRTEM images of (a) as-synthesized Ni/C product, (b) surface-cleaned Ni/C product, and (c) as-prepared Ni/C/PANI nanocapsules.

$$\mathrm{RL} = 20\log|(Z_{in}-Z_0)/(Z_{in}+Z_0)|, \quad (1)$$

where $Z_{in} = Z_0(\mu_r/\varepsilon_r)^{1/2}\tanh[j(2\pi fd/c)(\mu_r/\varepsilon_r)^{1/2}]$ is the input impedance of absorber, $Z_0 \sim 377\ \Omega$ is the characteristic impedance of air, and $c = 3\times10^8$ m/s is the velocity of light.

Figure 1(a) shows the HRTEM image of the Ni/C product synthesized by the modified arc-discharge method. It is seen that the Ni/C product contains both Ni/C nanocapsules and Ni oxides. The Ni/C nanocapsules own a typical core/shell structure in which Ni nanoparticle cores of ~4.6 nm diameter is encapsulated by a C onion-like shell of ~1.5 nm thickness. Due to the formation of Ni oxides on the surface of the C shell, surface cleaning of the as-synthesized Ni/C product in HCl aqueous solution was carried out prior to the coating of the second PANI shell using the chemical polymerization method. Nonetheless, the lattice plane spacing of the C shell is ~0.34 nm, corresponding to the (002) plane of graphite.[1,2] Lattice imperfection is observed in the C shell due to the bending and collapse of the atomic layer of graphite. Figure 1(b) illustrates the HRTEM image of the surface-cleaned Ni/C product. In addition to the core/shell-structured Ni/C nanocapsules described in Fig. 1(a), a few percent of cage-like C hollow spheres is detected because the HCl aqueous solution can dissolve the Ni cores of the Ni/C nanocapsules through the lattice imperfection in the C protective shell during surface cleaning. Figure 1(c) displays the HRTEM image of the Ni/C/PANI product prepared by the chemical polymerization method. The proposed core/shell/shell structure having a Ni nanoparticle core, a first C shell, and a second PANI shell is formed.

Figure 2(a) shows the f dependence of ε_r of the paraffin-bonded Ni/C/PANI nanocapsule absorbers. The real (ε_r') and imaginary (ε_r'') parts of ε_r mainly represent the amount of polarization and the level of energy dissipation, respectively. It is noted that ε_r'' is larger than ε_r' in the whole f range of measurement, and the result is essentially different from traditional nanocapsules with a core/shell structure, because PANI possesses an unusually high ε_r'' (~10) in this f range. Moreover, both ε_r' and ε_r'' spectra present a multidielectric resonance characteristic with three distinct resonance frequencies at 4.0, 8.0, and 14.6 GHz. Recalling that the dielectric loss in a material is mainly determined by electronic polarization, ionic polarization, and dipolar polarization.[7–10] Since the dielectric loss is usually weak in the microwave frequency range for both electronic and ionic polarizations, it lets us to have a speculation that the high dielectric loss in our absorbers is primarily caused by dipolar polarization in which an electromagnetic energy is irreversibly transformed to a Joule thermal energy. The process can be described by the Debye dipolar polarization as[10]

$$\varepsilon_r = \varepsilon_\infty + \frac{\varepsilon_s-\varepsilon_\infty}{1+j2\pi f\tau} = \varepsilon_r'(f) - j\varepsilon_r''(f), \quad (2)$$

where f is the frequency of the electromagnetic wave, τ is the relaxation time, ε_s is the stationary permittivity, and ε_∞ is the optical permittivity. $\varepsilon_r'(f)$ in Eq. (2) can be written to depend on $\varepsilon_r''(f)$ and f as

$$\varepsilon_r'(f) = \frac{\varepsilon_r''(f)}{2\pi f\tau - \varepsilon_\infty}. \quad (3)$$

From Eq. (3), if the dielectric loss is a consequence of dipolar polarization, the plot of ε_r' versus B_0 ($=\varepsilon_r''/f$) would be linear.

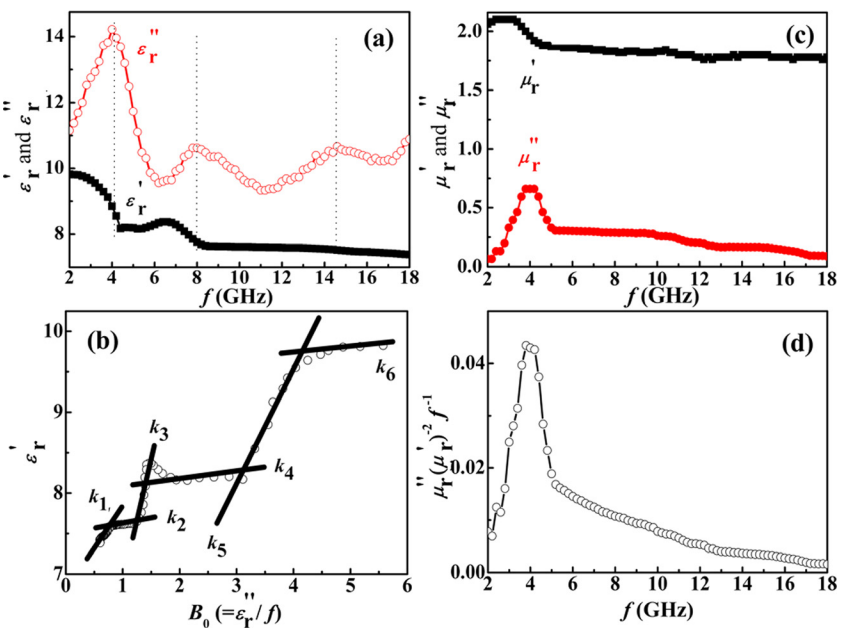

FIG. 2. Dielectric and magnetic properties of paraffin-bonded Ni/C/PANI nanocapsule absorbers. (a) ε_r' and ε_r'' versus f, (b) ε_r' versus B_0 ($=\varepsilon_r''/f$), (c) μ_r' and μ_r'' versus f, and (d) $\mu_r''(\mu_r')^{-2}(f)^{-1}$ versus f.

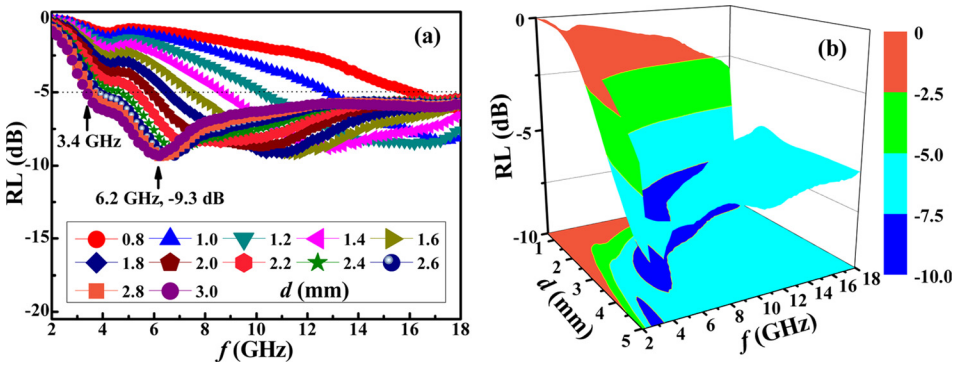

FIG. 3. RL as a function of f and d for paraffin-bonded Ni/C/PANI nanocapsule absorbers. (a) 2D and (b) 3D representations.

Figure 2(b) plots ε_r' versus B_0 for our absorbers. It is clear that there are six beelines with different slopes ($k = 1/2\pi\tau$) of $k_1 = 4.07$, $k_2 = 0.35$, $k_3 = 14.70$, $k_4 = 0.22$, $k_5 = 8.14$, and $k_6 = 0.32$. The results confirm the domination of the Debye-type dipolar polarization in our absorbers. The smaller values of k_2, k_4, and k_6 imply the existence of a longer relaxation time in the absorbers and also a higher difficulty for the Ni/C, C/PANI, and PANI/paraffin interfaces to get across the electric dipoles.[11,12] The frequencies of Debye dipolar polarization ($f_r = 1/2\pi\tau$), which are equal to the slopes of k_1, k_5, and k_3, are found to be 4.07, 8.14, and 14.70 GHz, respectively. These frequency values agree well with the measured multidielectric resonance frequencies of 4.0, 8.0, and 14.6 GHz in Fig. 2(a). Therefore, the dielectric loss in our absorbers is governed by the Debye-type multidielectric polarizations.

Figure 2(c) shows the f dependence of μ_r of the paraffin-bonded Ni/C/PANI nanocapsule absorbers. The real part of μ_r (μ_r') exhibits an initial drop from 2.1 to 1.87 in the 2–5 GHz range followed by a relatively stable trend of 1.8 in the 5–18 GHz range. The generally higher μ_r' in our absorbers compared to the traditional core/shell-structured nanocapsule absorbers suggests that the double shell structure is better than the traditional single shell structure in term of protection of magnetic cores at 2–18 GHz. The imaginary part of μ_r (μ_r'') has a strong peak at 4 GHz with a wide range of variation covering the 2–8 GHz range. This indicates the presence of a strong and broad magnetic natural resonance, as the major contributor to magnetic loss, in our absorbers. Other magnetic loss contributors, such as hysteresis loss, domain-wall displacement, and eddy-current loss, can be excluded in our absorbers. First, hysteresis loss mainly results from the time lag of the magnetization vector behind the external electromagnetic field vector and can be neglected in weak applied fields. Second, domain-wall displacement only occurs in multidomain magnetic materials and does not apply to our Ni/C/PANI nanocapsules of sizes smaller than a single magnetic domain (55 nm). Third, eddy-current loss should be supported by the skin-effect criterion in which $\mu_r''(\mu_r')^{-2}(f)^{-1}$ should be independent of f. As shown in Fig. 2(d), $\mu_r''(\mu_r')^{-2}(f)^{-1}$ of our absorbers gives a strong peak at 3.8 GHz and does not fulfill the skin-effect criterion. Thus, the magnetic loss in our absorbers is mainly due to magnetic natural resonance.[6]

Figure 3(a) shows the f dependence of RL at various d for the paraffin-bonded Ni/C/PANI nanocapsule absorbers. An optimal RL of −9.3 dB, corresponding to an absorption of ∼88%, is observed at 6.2 GHz for $d = 3.0$ mm. RL exceeding −5 dB, corresponding to an absorption of ∼68%, is found from 3.4 to 18 GHz for $d = 3.0$ mm. This −5 dB-bandwidth is as broad as 14.6 GHz, covering some of the S band (2–4 GHz) as well as the whole C band (4–8 GHz), X band (8–12 GHz), and Ku band (12–18 GHz). Besides, d can be varied in a very large range from 3.0 to 1.0 mm without deteriorating the optimal RL by 10% (−8.4 dB). For traditional core/shell-structured nanocapsules, RL is very sensitive to d and a very limited d range of ∼0.2 mm is generally obtained.[1–10] Figure 3(b) shows the 3D representation of Fig. 3(a). It is clear that when d is increased from 0.8 to 3 mm, the absorbing bandwidth becomes broader and the optimal RL shifts to the low-frequency side while remaining almost invariant in magnitude. This shows a physically interesting and practically useful characteristic of broadband absorption and large thickness range in our absorbers.

We have prepared core/shell/shell-structured Ni/C/PANI nanocapsules and evaluated their microwave absorbing properties in the full S–Ku bands. An investigation into ε_r and μ_r has confirmed Debye-type multidielectric polarizations and magnetic natural resonance as the major contributors of the dielectric and magnetic losses, respectively. The combination of the multidielectric polarizations and broad magnetic natural resonance has effectively extended the absorbing bandwidth and absorber thickness range by the bandwidth-broadening effect in various core/shell/shell material phases. A 3 mm-thick absorber has shown an optimal RL of −9.3 dB at 6.2 GHz, an extremely broad −5 dB-bandwidth of 3.4–18 GHz in almost the whole S–Ku bands, and a very large thickness range of down to 1 mm without deteriorating RL by 10%.

This work was supported by the Research Grants Council of the HKSAR Government (PolyU 5236/12E) and The Hong Kong Polytechnic University (G-YK59 and 4-ZZ7L).

[1]X. F. Zhang *et al.*, Appl. Phys. Lett. **89**, 053115 (2006).
[2]X. G. Liu *et al.*, Carbon **47**, 470 (2009).
[3]X. G. Liu *et al.*, Appl. Phys. Lett. **94**, 053119 (2009).
[4]X. G. Liu *et al.*, Mater. Res. Bull. **48**, 3887 (2013).
[5]X. G. Liu *et al.*, RSC Adv. **3**, 14590 (2013).
[6]X. L. Dong *et al.*, Appl. Phys. Lett. **92**, 013127 (2008).
[7]A. G. MacDiarmid, Synth. Met. **125**, 11 (2001).
[8]R. T. Ma *et al.*, Mater. Res. Bull. **45**, 1064 (2010).
[9]S. M. Abbas *et al.*, Mater. Sci. Eng. B **123**, 167 (2005).
[10]X. F. Zhang *et al.*, Appl. Phys. Lett. **96**, 223111 (2010).
[11]C. G. Koops, Phys. Rev. **83**, 121 (1951).
[12]D. Roy *et al.*, Chem. Phys. Lett. **373**, 52 (2003).